Journal of Molecular Liquids 200 (2014) 32–37

Contents lists available at ScienceDirect

Journal of Molecular Liquids

journal homepage: www.elsevier.com/locate/molliq

Theoretical analysis of salt effect on intramolecular proton transfer reaction of glycine in aqueous NaCl solution

Yukako Kasai, Norio Yoshida *, Haruyuki Nakano

Department of Chemistry, Graduate School of Sciences, Kyushu University, 6-10-1, Hakozaki, Higashi-ku, Fukuoka 812-8581, Japan

ARTICLE INFO

Article history:
Received 30 October 2013
Received in revised form 10 January 2014
Accepted 7 February 2014
Available online 28 February 2014

Keywords:
Intramolecular proton transfer
Glycine
Salt effect
RISM-SCF

ABSTRACT

The salt effect on the intramolecular proton transfer reaction of glycine in aqueous NaCl solution was considered using the reference interaction-site model self-consistent field theory. The free energy profiles were computed for various salt concentrations. The set of profiles clearly showed that the free energy gap between the zwitterionic form (ZW) and the neutral form (NF) became larger as the NaCl concentration increased. The transition-state structure of the solute glycine approaches the NF structure, and the reaction barrier height is reduced. From the energy decomposition analysis of the free energy of solvation, we found that the changes in the solvation free energy are determined by the balance between the electronic distortion energy, the electrostatic interaction, the solvent reorganization, and the entropic effects caused by the NaCl addition. The salt effect of NaCl makes all the species associated with the reaction unstable; however, the destabilization of NFs caused by NaCl addition is stronger than that of ZWs. In the ZW, the penalty coming from the solvent reorganization and the entropic effects are compensated by the strong solute–solvent electrostatic interaction.

1. Introduction

The salt effect on the solvation of molecules is one of the most important issues in the fields of chemistry, physics, and biochemistry [1]. The addition of an electrolyte to water enhances hydrophobic hydration and/or hydrophilic interaction [2].

In the present study, the salt effect on the intramolecular proton transfer of glycine in aqueous NaCl solution is considered theoretically. Glycine, the simplest amino acid, is used as a probe to understand the mechanism of the proton transfer in solution, and therefore a number of computational and theoretical studies on glycine-involving reactions have been conducted to clarify the solvent effects [3–6]. However, the salt effect has not previously been considered because of the difficulty in theoretical treatment of the electronic structure of molecules in the electrolyte solution.

To consider the salt effect in electrolyte solutions, two important solvent effects, hydrophobic and hydrophilic effects, should be considered carefully. Continuum solvent models, such as the polarizable continuum model and the generalized Born model, are inadequate in this respect, because they inherently disregard the molecularity of the solvent, and thus they cannot handle hydrophobicity [7]. On the other hand, molecular simulations such as the Monte-Carlo (MC) method and the molecular dynamics (MD) have difficulty in treating the salt effect for the reaction free energy, because the convergence of the sampling configuration space of ions in dilute salt concentration is extremely slow.

The reference interaction-site model self-consistent field (RISM-SCF) theory is a promising way to tackle the problem [8,9]. It can handle the salt effect from first principles without making any unwarranted assumptions concerning the solvent effects [10,11]. In this theory, the solvent effects on the solute electronic structure are considered by means of the RISM integral equation theory, which is a statistical mechanics theory of molecular liquids [12,13]. The RISM theory has been successfully applied to the investigation of various chemical and biological phenomena [14,15]. Imai et al. applied the RISM theory to the salt effect on the stability of peptide conformation to clarify the physical origin of the Hofmeister series [16]. Recently, one of the present authors applied the RISM theory to investigate ion binding by human lysozyme in LiCl, NaCl, KCl, and $CaCl_2$ aqueous solutions [17,18]. In these papers, selective ion binding by a variety of mutants of human lysozyme was well reproduced, in good agreement with corresponding experiments. In their calculations, the mean activity coefficients of electrolyte solutions, which are the most fundamental physicochemical properties characterizing electrolyte solutions, were reproduced reasonably well. Those applications demonstrate unequivocally that the RISM (and therefore RISM-SCF) theory can be applied to the investigation of the salt effect on chemical and physical phenomena in the solution.

In the present study, we employ the RISM-SCF theory to investigate the intramolecular proton transfer reaction of glycine between its neutral form (NF) and zwitterionic form (ZW) in both water and NaCl aqueous solutions at various concentrations (Scheme 1). A stationary-point search was also performed to find the transition state (TS) structure. The free energy change and the barrier height of the reaction were evaluated. At all reaction steps (TS, NF, and ZW), the geometry of the glycine

* Corresponding author. Tel./fax: +81 92 642 2588.
E-mail address: noriwo@chem.kyushu-univ.jp (N. Yoshida).

http://dx.doi.org/10.1016/j.molliq.2014.02.013
0167-7322/

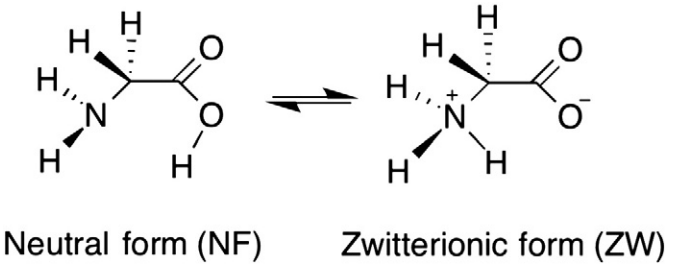

Scheme 1. Scheme of the intra-molecular proton transfer reaction of glycine.

was optimized using the analytical free energy gradients of the RISM-SCF free energy formula [9]. The solvation structures of glycine were also considered to probe the salt effect.

2. Computational methods

2.1. Brief overview of the RISM-SCF method

The RISM-SCF method combines electronic structure theory and integral equation theory. It was initially developed by Ten-No, Hirata, and Kato [8]. The solvated molecule is treated using quantum chemistry, whereas the surrounding solvent molecules are treated using statistical mechanics.

Assuming a molecule in solution at infinite dilution, the Helmholtz free energy A of the solute–solvent system is given as the sum:

$$A = E_{\text{solute}} + \Delta\mu, \tag{1}$$

where E_{solute} is the solute electronic energy computed from quantum chemical electronic structure theory and $\Delta\mu$ is the excess chemical potential from the solute–solvent interaction. In the RISM-SCF method, the excess chemical potential is computed from the number density of the solvent ρ_ν and the interaction potential between the solute molecule and solvent site γ:

$$\Delta\mu = 4\pi\sum_{\nu}\rho_\nu\int_0^1 d\lambda\int dr\sum_{\alpha}\sum_{\gamma} r^2\lambda u_{\alpha\gamma}(r)g^{\lambda}_{\alpha\gamma}(r), \tag{2}$$

where $g^{\lambda}_{\alpha\gamma}(r)$ and $u_{\alpha\gamma}(r)$ denote the radial distribution function and solute–solvent interaction potential, respectively. If we employ Kovalenko–Hirata (KH) closure [19,20]:

$$h_{\alpha\gamma}(r) = \begin{cases} \exp\left\{-\beta u_{\alpha\gamma}(r) + h_{\alpha\gamma}(r) - c_{\alpha\gamma}(r)\right\} - 1 & \text{for} \quad h_{\alpha\gamma}(r) < 0 \\ -\beta u_{\alpha\gamma}(r) + h_{\alpha\gamma}(r) - c_{\alpha\gamma}(r) & \text{for} \quad h_{\alpha\gamma}(r) \geq 0 \end{cases}, \tag{3}$$

the integration about λ in Eq. (2) can be performed analytically, where u denotes the site–site interaction potential, which is the sum of the Lennard–Jones potential and Coulomb interaction. As a result, Eq. (2) becomes:

$$\Delta\mu = 4\pi\sum_{\nu}\rho_\nu k_B T\sum_{\alpha}\sum_{\gamma}\int dr \times\left[\left(h_{\alpha\gamma}(r)\right)^2\theta\left(-h_{\alpha\gamma}(r)\right)/2 - c_{\alpha\gamma}(r) - h_{\alpha\gamma}(r)c_{\alpha\gamma}(r)/2\right]r^2. \tag{4}$$

Here, k_B is the Boltzmann constant, T is the absolute temperature, and $\theta(x)$ is the Heaviside step function. Functions $h_{\alpha\gamma}$ and $c_{\alpha\gamma}$ are the site–site total and direct correlation functions, respectively.

The Helmholtz free energy is a functional of the electronic wave function $\varphi(\mathbf{r})$ (or electronic density in density functional theory, DFT) of the solute molecule, and the correlation functions h and c: $A = A[\varphi(\mathbf{r}), h, c]$. The basic equations of the RISM-SCF method are derived by the variation of the free energy, Eq. (1), with respect to the electronic wave function (or the electron density in DFT) and the correlation functions h and c [19]. If we adopt the Kohn–Sham DFT for the solute electronic structure theory, the resulting equation for the solute molecules is the Kohn–Sham equation (KS) for the KS operator f that includes the interaction from the solvent molecules:

$$f\varphi(\mathbf{r}) = \varepsilon\varphi(\mathbf{r}), \tag{5}$$

where ε and $\varphi(\mathbf{r})$ are the orbital energy and the KS orbital, respectively. The equations for the solvent are the KH closure relation, Eq. (3), and the site–site Ornstein–Zernike (OZ) equation:

$$h(r) = \omega(r) * c(r) * (\omega(r) + \rho_\nu h(r)), \tag{6}$$

where ω, with matrix elements $\omega_{\alpha\gamma}(r) = \delta(r - l_{\alpha\gamma})$, is the intramolecular correlation matrix of a solvent molecule with site separation $l_{\alpha\gamma}$, and the operation symbol * means convolution in direct space. These basic Eqs. (3), (5), and (6) are coupled with each other via the interaction potentials between the solute and solvent molecules.

2.2. Computational details

We used the RISM-SCF theory to estimate the free energies, the geometry, the electronic structures, and the solvent distribution of glycine immersed in aqueous NaCl solution at infinite dilution. The free energy of the system is evaluated for the NF, ZW, and TS structures.

The electronic structure method for the solute molecules used in the RISM-SCF method was DFT with the M06-2X functional [21]. The basis set used was 6–31++G**. The parameters used in the RISM-SCF methods were as follows. The temperature was 298 K. The calculations were carried out in the range of concentrations at 0.0–10.0 M, and we chose pure water, 0.1 M, 5.0 M, and 10.0 M NaCl solutions. 0.1 M is close to physiological conditions and 5.0 M is close to saturated solution. To examine the extreme condition, 10.0 M was chosen. We note that the 10.0 M solution is an imaginary condition because it is much higher than the saturation concentration. The number density of the components of the solution is determined computationally, where we assumed that the volumes of water molecules and ions are identical to those for the saturated solution. Effective point charges were employed to describe the solute–solvent interaction potential. The effective point charges on the solute molecule were determined so as to reproduce the electrostatic potential around the solute molecule by using least-squares fitting. The Lennard–Jones parameters for the solute amino acid were taken from the OPLSAA parameter set [22]. The simple point-charge model (SPC) parameter set for the geometrical and potential parameters for the solvent water was employed with modified hydrogen parameters ($\sigma = 1.0$ Å and $\varepsilon = 0.056$ kcal mol^{-1}) [23]. The OPLSAA parameter set for solvent ions was employed. The number of grid points in the RISM-SCF calculations was 2048 with a spacing of 0.01 Å.

All of the calculations were performed with a modified version of the GAMESS program package [24], in which the RISM-SCF and its gradient methods were implemented [25].

3. Results and discussion

3.1. Free energy profiles of proton transfer

We examine the free energy profiles for the reaction from the NF to ZW via TS in various concentrations of NaCl electrolyte solution.

In Fig. 1, the free energy changes from the NF are depicted. In water, the free energy of the ZW is 10.5 kcal mol^{-1} lower than that of the NF. This result is comparable with previous experimental and theoretical results [4,5,26,27]. The barrier is only 1.3 kcal mol^{-1} in water, which is also in good agreement with previous calculations. The magnitude of stabilization of the ZW increases with the addition of NaCl electrolyte to the water: the reaction free energies from the NF are −10.8, −12.6,

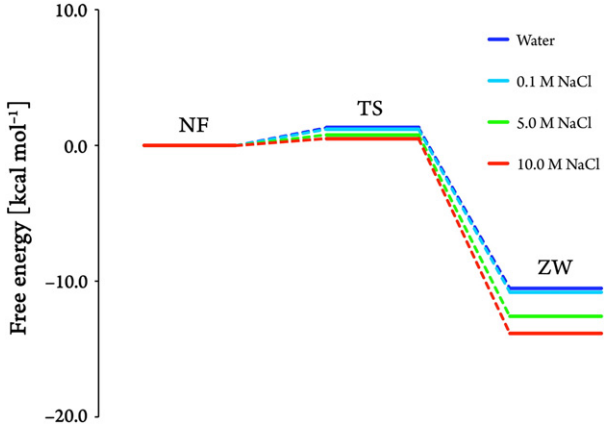

Fig. 1. Free energy profile of intramolecular proton transfer compared in different NaCl concentrations. NF, TS, and ZW mean neutral form, transition state, and zwitterionic form, respectively.

and −13.9 kcal mol^{-1} in 0.1, 5.0, and 10.0 M NaCl solutions. The free energies of the TS stabilize with increasing NaCl concentration.

In Table 1, the structural parameters are summarized. In both the NF and ZW structures, the structural changes caused by the NaCl addition are very small, 0.01–0.02 Å, whereas those in the TS structure are relatively large, 0.03–0.05 Å. In the TS structure, the distance between N and H, R(N–H), increases, while that between O and H, R(O–H), decreases. This means that the TS structure approaches the NF structure with the addition of NaCl.

The solvation free energy is defined as the sum of the electronic energy change, ΔE_{solute}, and excess chemical potential, $\Delta\mu$:

$$\Delta A = \Delta E_{solute} + \Delta\mu. \tag{7}$$

The solvation free energy and its components are summarized in Table 2. The electronic energy change is defined as:

$$\Delta E_{solute} = E_{solute} - E_{gas}, \tag{8}$$

where E_{gas} is the gas-phase energy of glycine for the NF structure. Note that the glycine can take only the NF structure in the gas phase. ΔE_{solute} includes the electronic distortion energy from the solute–solvent interaction and the energy changes caused by the structural changes, such as proton transfer, namely:

$$\begin{aligned} \Delta E_{solute} &= \Delta E_{gas} + \Delta E_{dist} \\ \Delta E_{struct} &= E_{gas}(\mathbf{r}_{solute}) - E_{gas}\left(\mathbf{r}_{gas}\right), \\ \Delta E_{dist} &= E_{solute}(\mathbf{r}_{solute}) - E_{gas}(\mathbf{r}_{solute}) \end{aligned} \tag{9}$$

where $\mathbf{r}_{solute}$ and $\mathbf{r}_{gas}$ denote the coordinates of solute atoms optimized in the solution and gas phases, respectively. The excess chemical potential $\Delta\mu$ can also be decomposed into the solute–solvent interaction energy, E_{uv}, the solvent reorganization energy, E_{vv}, and the solvation entropy, ΔS [11,14,28]:

$$\Delta\mu = E_{uv} + E_{vv} - T\Delta S, \tag{10}$$

where the solute–solvent interaction energy is given by

$$E_{uv} = 4\pi \sum_{\nu} \rho_{\nu} \sum_{\alpha\gamma} \int u_{\alpha\gamma}(r) g_{\alpha\gamma}(r) r^2 dr, \tag{11}$$

and the remaining components of the excess chemical potential, namely the sum of solvent reorganization and entropy term, can be evaluated as $E_{vv} - T\Delta S = \Delta\mu - E_{uv}$. The components of ΔE_{solute} and $\Delta\mu$ are summarized in Tables 3 and 4, respectively. The tables show that, in pure water, the ZW glycine is stabilized by solvation, whereas the NF glycine is

Table 1
Structural properties.[a]

	NF		TS		ZW	
Solvent	R(N–H)	R(O–H)	R(N–H)	R(O–H)	R(N–H)	R(O–H)
Water	1.82	1.00	1.34	1.18	1.04	2.01
0.1 M NaCl	1.81	1.00	1.35	1.18	1.04	2.02
5.0 M NaCl	1.81	1.00	1.37	1.17	1.04	2.03
10.0 M NaCl	1.80	1.01	1.39	1.15	1.04	2.03

[a] Units are given in Å.

Table 2
Solvation free energy and its components.[a]

	NF–NF^{gas}			ZW–NF^{gas}		
Solvent	ΔA	ΔE_{solute}	$\Delta\mu$	ΔA	ΔE_{solute}	$\Delta\mu$
Water	2.1	10.4	−8.3	−8.5	53.2	−61.6
0.1 M NaCl	2.1	10.5	−8.5	−8.7	54.0	−62.8
5.0 M NaCl	8.9	11.7	−2.7	−3.7	57.0	−60.7
10.0 M NaCl	22.2	12.6	9.6	8.4	58.8	−50.4

[a] Units are in kcal mol^{-1}.

Table 3
Components of solute energy change.[a]

	NF			ZW		
Solvent	ΔE_{solute}	ΔE_{struct}	ΔE_{dist}	ΔE_{solute}	ΔE_{struct}	ΔE_{dist}
Water	10.4	1.3	9.1	53.2	28.4	24.8
0.1 M NaCl	10.5	1.4	9.1	54.0	28.7	25.3
5.0 M NaCl	11.7	1.5	10.1	57.0	29.1	28.0
10.0 M NaCl	12.6	1.7	10.9	58.8	29.3	29.5

[a] Units are given in kcal mol^{-1}.

Table 4
Components of excess chemical potential.[a]

	NF			ZW		
Solvent	$\Delta\mu$	E_{uv}	$E_{vv} - T\Delta S$	$\Delta\mu$	E_{uv}	$E_{vv} - T\Delta S$
Water	−8.3	−65.3	57.0	−61.6	−170.1	108.5
0.1 M NaCl	−8.5	−65.8	57.3	−62.8	−172.4	109.6
5.0 M NaCl	−2.7	−69.8	67.1	−60.7	−182.3	121.6
10.0 M NaCl	9.6	−71.9	81.5	−50.4	−186.6	136.2

[a] Units are given in kcal mol^{-1}.

Table 5
Atomic components of solvation free energy difference between NF and ZW.[a]

	$\Delta\Delta\mu_x$[c]			
x[b]	H_2O	0.1 M NaCl aq.	5 M NaCl aq.	10 M NaCl aq.
N1	4.5	4.5 (0.0)	5.0 (0.5)	5.6 (1.1)
H2	−5.3	−5.4 (−0.1)	−6.0 (−0.8)	−6.6 (−1.3)
H3	−6.1	−6.2 (−0.1)	−6.8 (−0.7)	−7.2 (−1.1)
H4	−5.9	−5.9 (0.0)	−6.5 (−0.6)	−6.9 (−1.0)
C5	−2.2	−2.2 (0.0)	−2.8 (−0.6)	−3.5 (−1.3)
C6	18.7	18.9 (0.2)	20.7 (2.0)	21.8 (3.1)
O7	−24.9	−25.6 (−0.7)	−28.0 (−3.0)	−28.5 (−3.6)
O8	−33.3	−33.3 (.0)	−34.7 (−1.3)	−35.9 (−2.6)
H9	0.4	0.4 (0.0)	0.5 (0.1)	0.6 (0.2)
H10	0.4	0.4 (.0)	0.5 (0.1)	0.5 (0.1)
Total	−53.3	−54.3 (−1.0)	−58.0 (−4.7)	−60.0 (−6.7)

[a] Units are given in kcal mol^{-1}.
[b] Labels of solute atoms are defined in Fig. 2.
[c] Numbers in parentheses denote the difference of $\Delta\Delta\mu_x$ from those in H_2O.

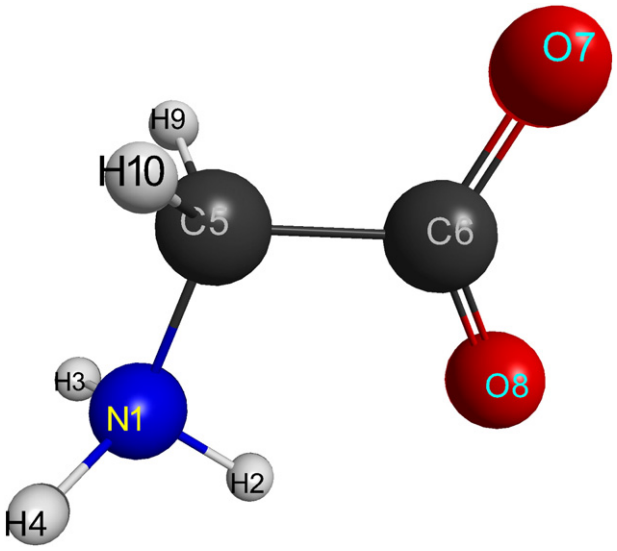

Fig. 2. Definition of the labels for solute atoms.

destabilized. For the ZW, $\Delta\mu$ has a large negative value, while ΔE_{solute} is positive. This implies that the strong solute–solvent electrostatic interactions contribute to the stabilization, giving positive electronic distortion energy. On the other hand, the NF glycine shows only small changes in both ΔE_{solute} and $\Delta\mu$; this is because the polarity of the NF glycine is relatively small compared with that of the ZW, and as a result, the structural change of glycine from the gas phase is small.

The NaCl addition increases the solvation free energy both in the ZW and NF. The major factor in this increase is the increase in the excess chemical potential. Although the stabilization of the solute–solvent interaction energy is enhanced, the solvent reorganization and entropic terms are increased. Increasing these terms makes the change of $\Delta\mu$ positive in total. In addition, the enhanced solute–solvent interactions distort the electronic structure of the solute glycine; as a result, the ΔE_{solute} increases with NaCl addition. By all these factors, the magnitude of the increase in the free energy of the ZW state by the NaCl addition is smaller than that of NF and consequently, the free energy gap of proton transfer increases with NaCl addition.

3.2. Solvation structure

To consider the microscopic picture of the solvation structure, we investigated the radial distribution functions (RDFs) and the atomic components of the excess chemical potential.

The atomic components of excess chemical potential difference between the NF and ZW, $\Delta\Delta\mu_x$, are summarized in Table 5. This quantity, $\Delta\Delta\mu_x$, is defined as:

$$\Delta\Delta\mu_x = \Delta\mu_x^{ZW} - \Delta\mu_x^{NF}, \tag{12}$$

where $\Delta\mu_x^{ZW}$ and $\Delta\mu_x^{NF}$ denote the atomic components of the excess chemical potential of solute atom x at ZW and NF, respectively. From Eq. (4), the atomic components of the solvation free energy $\Delta\mu_x$ can be defined as:

$$\Delta\mu = \sum_{x}^{\text{Solute atoms}} \Delta\mu_x. \tag{13}$$

As can be seen in Table 5, three amino hydrogens (H2, H3, and H4) and two carbonyl oxygens (O7 and O8) contribute to the stabilization

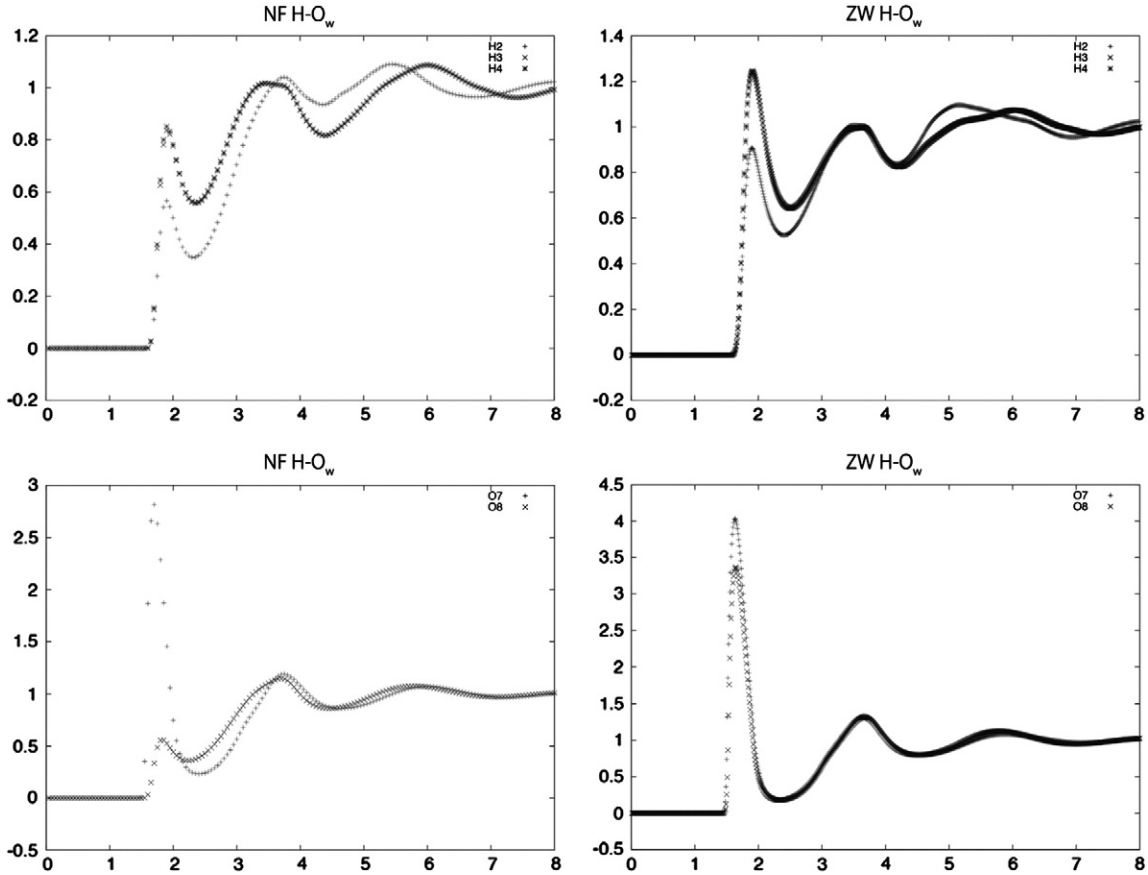

Fig. 3. Radial distribution functions between the solute and solvent water are plotted against site separation. Horizontal axes are given in angstroms.

of the ZW, whereas the amino nitrogen and the carbonyl carbon destabilize the ZW in solution; the labels of the solute atoms are defined in Fig. 2. In the upper panels of Fig. 3, the RDFs between solute H and solvent water oxygen, O_w, are depicted. The first peaks of the RDFs become higher because of the proton transfer from the NF to ZW. The stronger interactions between the amino hydrogen and solvent oxygen in the ZW state are a major factor in the negative values of $\Delta\Delta\mu$: H2 shows a smaller change than H3 and H4, because the interaction between H2 and the solvent is weakened by the steric hindrance of O8. In the lower panels of Fig. 3, the RDFs between solute carbonyl O and solvent water hydrogen, H_w, are depicted. In the ZW state, both O7 and O8 show a conspicuous peak at 1.8 Å. In contrast, the first peak of the RDF of O8–H_w is weaker in the NF state, because O8 forms bond with H2. The solvation structure of O8 changes drastically with the proton transfer, and consequently, $\Delta\Delta\mu_{O8}$ is much larger than $\Delta\Delta\mu_{O7}$. The positive values of $\Delta\Delta\mu$ of N1 and C6 may be attributed to the electrostatic repulsion from the solvent coordinated around the adjacent carbonyl oxygen and amino hydrogen, respectively.

In NaCl solution, the behavior of $\Delta\Delta\mu$ is qualitatively similar to that in pure water, while the magnitudes of the $\Delta\Delta\mu$ values increase slightly as the NaCl concentration increases. The most remarkable change is seen for O8. The RDFs between O8 and positively charged solvent atoms are depicted in Fig. 4, and the excess chemical potential and the solute–solvent interaction energy are summarized in Table 6. Here, the solute–solvent interaction energy of O8 atom can be defined as:

$$E_{uv}^{O8} = 4\pi\sum_{v}\rho_v\sum_{\gamma}\int u_{O8\text{-}\gamma}(r)g_{O8\text{-}\gamma}(r)r^2dr\times \tag{14}$$

Table 6
Excess chemical potential, solute–solvent interaction energy of O8 site and the coordination number of Na^+ at first solvation shell.

	State	Water	0.1 M	5.0 M	10.0 M
$\Delta\mu_{O8}$[a]	NF	−6.4	−6.5	−5.0	−2.7
	ZW	−39.5	−39.7	−39.7	−38.7
$E^{O8}{}_{uv}$[a]	NF	−18.2	−18.3	−18.6	−19.0
	ZW	−79.2	−79.6	−81.0	−82.2
CN[b]	NF	0.00	0.003	0.18	0.38
	ZW	0.00	0.01	0.50	0.90

[a] Units are given in kcal mol^{-1}.
[b] Units are given in molecules.

$E^{O8}{}_{uv}$ decreases as the NaCl concentration increases for both NF and ZW, because the solute–solvent electrostatic interactions are enhanced. $\Delta\mu_{O8}$ decreases at 0.1 M but increases with higher NaCl concentrations. This indicates that $\Delta\mu_{O8}$ is determined by the balance between the solute–solvent interaction, the solvent reorganization, and the entropic term from the NaCl addition. Therefore, the solvent reorganization and entropic terms are dominant for high concentrations of NaCl. In Fig. 4, the first peak of the positively charged solvent sites increases with the increase in NaCl concentration for the NF, whereas the ZW shows the opposite behavior. Apparently, this behavior of RDFs in the ZW seems to contradict the enhancements of the solute–solvent interaction. However, as can be seen in Eq. (14), the solute–solvent interaction energy is determined not only by RDFs but also by the density of the solvent and the solute–solvent interaction potential. In fact, the coordination number of Na^+ around the O8 atom increases as the NaCl concentration increases (see Table 6). Similar analysis can be performed for all the other pairs of solute atoms and solvent sites but is not shown here.

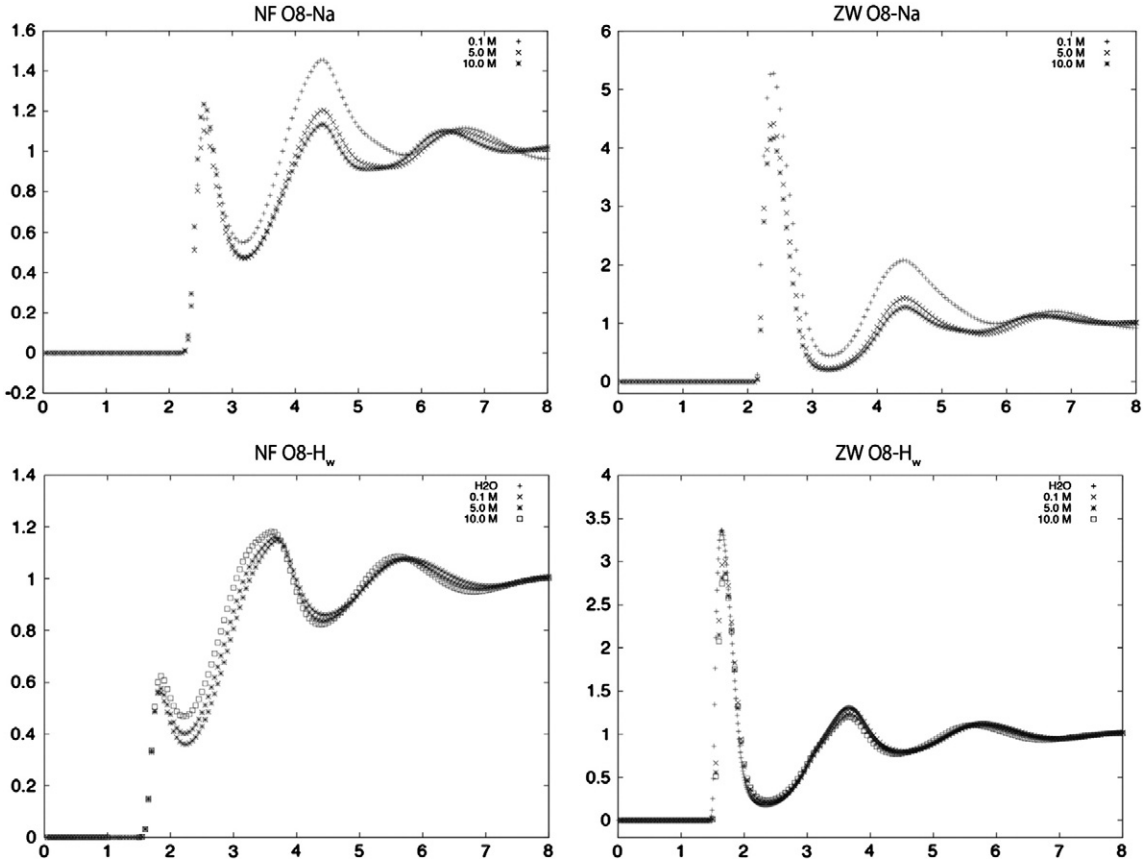

Fig. 4. Radial distribution function between solute O8 and positively charged site of solvent for different NaCl concentrations is plotted against the site separation. Horizontal axes are given in angstroms.

4. Conclusion

We have considered the salt effect on the intramolecular proton transfer reaction of glycine in aqueous NaCl solution using the RISM-SCF theory.

The free energy profiles were computed for various salt concentrations and solvation structures by means of radial distribution functions. The set of profiles clearly showed that the proton transfer reaction from the NF to ZW becomes more exothermic, and the activation energy (or barrier height) of the reaction reduces on adding NaCl. The TS structure of the reaction approaches the NF structure, and the reaction barrier is reduced. From the energy decomposition analysis of the free energy of solvation, we found that a major factor in the solvation free energy changes is the increased solvent reorganization and entropic term because of the NaCl addition. The salt effect of NaCl destabilizes all species. However, the destabilizations of the NF caused by NaCl addition are stronger than those of the ZW. In the ZW, the salt effects are suppressed by enhancing the electrostatic interactions between the solute and the solvent.

Acknowledgments

This work was partially supported by Grants-in-Aid for Scientific Research (Nos. 23550018, 24655018, and 25410021) from the Ministry of Education, Culture, Sports, Science and Technology in Japan. N.Y. is grateful to the Strategic Programs for Innovative Research (SPIRE), the Computational Materials Science Initiative (CMSI), Japan, and a grant from the Sumitomo Foundation.

References

[1] K.D. Collins, G.W. Neilson, J.E. Enderby, Biophys. Chem. 128 (2007) 95.
[2] D.C. Rideout, R. Breslow, J. Am. Chem. Soc. 102 (1980) 7816.
[3] I. Adamovic, M.A. Freitag, M.S. Gordon, J. Chem. Phys. 118 (2003) 6725.
[4] J.H. Jensen, M.S. Gordon, J. Am. Chem. Soc. 117 (1995) 8159.
[5] N. Takenaka, Y. Kitamura, Y. Koyano, T. Asada, M. Nagaoka, Theor. Chem. Acc. 130 (2011) 215.
[6] Q. Cui, J. Chem. Phys. 117 (2002) 4720.
[7] J. Tomasi, M. Persico, Chem. Rev. 94 (1994) 2027.
[8] S. Ten-No, F. Hirata, S. Kato, J. Chem. Phys. 100 (1994) 7443.
[9] H. Sato, F. Hirata, S. Kato, J. Chem. Phys. 105 (1996) 1546.
[10] F. Hirata (Ed.), Molecular Theory of Solvation, Kluwer, Dordrecht, 2003.
[11] N. Yoshida, H. Tanaka, F. Hirata, J. Phys. Chem. B 117 (2013) 14115.
[12] D. Chandler, H.C. Andersen, J. Chem. Phys. 57 (1972) 1930.
[13] F. Hirata, P.J. Rossky, J. Chem. Phys. 74 (1981) 5324.
[14] T. Imai, M. Kinoshita, F. Hirata, J. Chem. Phys. 112 (2000) 9469.
[15] N. Yoshida, T. Imai, S. Phongphanphanee, A. Kovalenko, F. Hirata, J. Phys. Chem. B 113 (2009) 873.
[16] T. Imai, M. Kinoshita, F. Hirata, Bull. Chem. Soc. Jpn. 73 (2000) 1113.
[17] N. Yoshida, S. Phongphanphanee, Y. Maruyama, T. Imai, F. Hirata, J. Am. Chem. Soc. 128 (2006) 12042.
[18] N. Yoshida, S. Phongphanphanee, F. Hirata, J. Phys. Chem. B 111 (2007) 4588.
[19] A. Kovalenko, F. Hirata, J. Chem. Phys. 110 (1999) 10095.
[20] A. Kovalenko, F. Hirata, Chem. Phys. Lett. 349 (2001) 496.
[21] Y. Zhao, D.G. Truhlar, Theor. Chem. Acc. 120 (2008) 215.
[22] W.L. Jorgensen, D.S. Maxwell, J. TiradoRives, J. Am. Chem. Soc. 118 (1996) 11225.
[23] B. Pullman (Ed.), Intermolecular Forces, Reidel, Dordrecht, 1981.
[24] M.W. Schmidt, K.K. Baldridge, J.A. Boatz, S.T. Elbert, M.S. Gordon, J.H. Jensen, S. Koseki, N. Matsunaga, K.A. Nguyen, S. Su, T.L. Windus, M. Dupuis, J.A. Montgomery, J. Comput. Chem. 14 (1993) 1347.
[25] N. Yoshida, F. Hirata, J. Comput. Chem. 27 (2006) 453.
[26] G. Wada, E. Tamura, M. Okina, M. Nakamura, Bull. Chem. Soc. Jpn. 55 (1982) 3064.
[27] C.H. Choi, S. Re, M. Feig, Y. Sugita, Chem. Phys. Lett. 539–540 (2012) 218.
[28] H.A. Yu, M. Karplus, J. Chem. Phys. 89 (1988) 2366.